Threshold Effects in Electron Transfer to Oriented Molecules

Guoqiang Xing,[1] Toshio Kasai,[2] and Philip R. Brooks*

Contribution from the Chemistry Department and Rice Quantum Institute, Rice University, Houston, Texas 77251

Received September 30, 1994[⊗]

Abstract: The effects of molecular orientation on electron transfer are explored in collisions between haloalkane molecules oriented in molecular beams and K atoms which have sufficient energy to allow the charged products to separate. For several molecules studied (CF_3Br, CF_3Cl, and CH_3Br) attack at the "heads" end of the molecule (the end with the most weakly bound atom) always produces more K^+ ions. The effect of orientation is most dramatic at energies near threshold (≈5 eV) and disappears at energies of ≈20 eV, showing that steric requirements are energy dependent. Heads orientation has a lower energy threshold than tails orientation so there is a limited energy region where reaction occurs *only* in the heads orientation. For CF_3Br, the thresholds are 3.4 and 4.0 eV, corresponding to energies required for formation of CF_3Br^- and $CF_3 + Br^-$, respectively. For energies between 3.4 and 4.0 eV, reaction occurs only for attack at the Br end to form only two species, suggesting that the electron is preferentially transferred to the Br end of the molecule.

I. Introduction

Chemical reaction usually involves nonspherical molecules, and reactivity is widely believed to be localized or restricted to specific locations on the surface of the molecule. This notion was advanced by the ancient Greeks, is supported by molecular structural data and chemical "intuition", and is represented in various reaction rate theories as a "steric factor" or "entropy of activation".[3] But, since all possible molecular orientations are present in normal circumstances, experimental studies of steric effects have been limited to some clever rate vs substituent measurements which, for example, established the Walden inversion in S_N2 reactions.[4]

Orientation effects in thermal energy reactions have been directly observed in crossed molecular beam studies.[5] In the early studies (and those reported here) symmetric top molecules (CX_3Y) are state-selected and then oriented in a weak electric field.[6] Reactions studied include[7]

$$M + CH_3I \rightarrow MI + CH_3 \quad (M = K, Rb) \qquad (1)$$

$$K + CF_3X \rightarrow KX + CF_3 \quad (X = Br, I) \qquad (2)$$

In these cases the "heads" end of the molecule (the end with the weakest C−X bond) is more reactive, and for Rb + CH_3I the experimental data were interpreted[8] in terms of a cone of no reaction at the CH_3 end with half angle of ≈51°. Reaction 2 stands in striking contrast to reaction 1 in that *both* ends are reactive, but the angular distribution (and the mechanism) of the reactively scattered KX is different for heads or tails orientation.[9] For CF_3I the results can be explained by an impulsive "harpoon" model[10] consisting of the following steps:

$$K + CF_3I \rightarrow K^+ + CF_3I^- \quad \text{electron transfer} \qquad (3a)$$

$$CF_3I^- \rightarrow CF_3 + I^- \quad \text{molecular ion decomposition} \qquad (3b)$$

$$K^+ + I^- \rightarrow KI \quad \text{ion recombination} \qquad (3c)$$

The negative ion resulting from the electron transfer is probably formed either in a repulsive state or high on the repulsive wall of a bound state, so the molecular ion will dissociate within one vibration. The ejection of particles is thus similar to that which is obtained from photodissociation, picturesquely described in trajectory calculations as "direct interaction with product repulsion, distributed as in photodissociation" (DIPR-DIP).[11] This impulsive description almost completely accounts for the experimental results for oriented CF_3I,[12] suggesting that the orientation information is mostly contained in the molecular ion decomposition of step 3b above. But in contrast to the CF_3I results, in which heads and tails were roughly equally reactive, the tails orientation of CF_3Br is less reactive,[13] suggesting that the electron transfer step 3a might also be orientation dependent.

⊗ Abstract published in *Advance ACS Abstracts,* February 1, 1995.

(1) Present Address: Chemistry Department, Columbia University, New York, NY 10027.

(2) Permanent address: Laboratory of Chemical Kinetics, Chemistry Department, Faculty of Science, Osaka University, Toyonaka, Osaka, Japan.

(3) See for example: (a) Bernstein, R. B. *Chemical Dynamics vis Molecular Beam and Laser Techniques*; Oxford University Press: New York, 1982. (b) Laidler, K. J. *Chemical Kinetics*, 3rd ed.; Harper & Row: New York, 1987.

(4) For example: (a) Streitweiser, A.; Heathcock, C. H.; Kosower, E. M. *Introduction to Organic Chemistry*, 4th ed.; McMillen: New York, 1992. (b) Gould, E. S. *Mechanism and Structure in Organic Chemistry*; Holt: New York, 1959.

(5) For reviews see: (a) Brooks, P. R. *Science* **1976**, 193, 11−16. (b) Bernstein, R. B.; Herschbach, D. R.; Levine, R. D. *J. Phys. Chem.* **1987**, 91, 5365. (c) Parker, D. H.; Bernstein, R. B. *Annu. Rev. Phys. Chem.* **1989**, 40, 561−595. (d) Stolte, S. *Atomic and Molecular Beam Methods*; G. Scoles, Ed.; Oxford: New York, 1988; Vol. 1, pp 631−652.

(6) Alternative "brute force" methods have been developed for orienting molecules in strong fields where $E_{rot} \ll \mu E$ and requires either very cold molecules or very high fields, but it is the only method available for orienting Σ-state molecules. For these Σ-state molecules, various optical methods described in ref 5b have been used to produce *polarization*, where the plane of rotation is selected, but one end is not distinguished from the other. See: (a) Loesch, H. J.; Remscheid, A. *J. Chem. Phys.* **1990**, *93*, 4779. (b) Friedrich, B.; Herschbach, D. R. *Z. Phys.* **1991**, *D18*, 153.

(7) Other reactions have been studied using oriented molecules. See references to Ba + N_2O, NO + O_3, and Ca* + CH_3F (summarized in: (a) Janssen, M. H. M.; Parker, D. H.; Stolte, S. *J. Phys. Chem.* **1991**, *95*, 8142−8153) and Ar* + CF_3H ((b) Ohoyama, H.; Iguro, T.; Kasai, T.; Kuwata, K. *Chem. Phys. Lett.* **1993**, *209*, 361−366).

(8) Bernstein, R. B. *J. Chem. Phys.*, **1985**, *82*, 3656.

(9) Brooks, P. R. *Faraday Discuss. Chem. Soc.* **1973**, *55*, 299.

(10) Herschbach, D. R. *Adv. Chem. Phys.* **1966**, *10*, 319.

(11) Kuntz, P. J.; Mok, M. H.; Polanyi, J. C. *J. Chem. Phys.* ***1969***, *50*, 4623. Herschbach, D. R. *Faraday Discuss. Chem. Soc.* ***1973***, *55*, 233.

(12) Brooks, P. R. *J. Phys. Chem.* **1993**, *97*, 2153−2157.

(13) Carman, H. S.; Harland, P. W.; Brooks, P. R. *J. Phys. Chem.* **1986**, *90*, 944−948.

0002-7863/95/1517-2581$09.00/0

Since electron transfer is a ubiquitous process of importance not only to the harpoon mechanism but also to many other processes, ranging from redox reactions in solution to photosynthesis, we have recently initiated studies[14] of how molecular orientation affects this process.

At thermal energies most reactions, such as those discussed above, form neutral products, and the effects of electron transfer must somehow be inferred from the overall process described in reaction 3. If enough energy is available, however, the intermediate *charged* particles can separate and be detected, so the electron transfer process itself can be probed a bit more directly. Thus, the electron transfer, reaction 3a, has been studied[15] for some simple (unoriented) systems using fast alkali atoms which have enough energy, ≈5 eV, to allow the ions to overcome the Coulomb attraction and to separate. Our preliminary hyperthermal atom studies with oriented molecules[14] show that orientation makes a large difference in the reactivity, with more K^+ ions being formed for heads orientation regardless of the dipole polarity of the heads end of the molecule. Thus reaction is more complicated than simply being restricted to the positive end of the dipolar molecule.

Unfortunately, the mere observation of ion formation does not allow us to draw conclusions about the orientation dependence of the *electron transfer*. The experiments probe the entire reaction process, which includes not only the entrance channel of the reaction, where electron transfer is expected, but also the exit channel where the products separate. The early experiments were mostly at energies of ca. 7−25 eV where the CX_3Y^- molecular ion was expected to impulsively dissociate into CX_3 and Y^-, giving as products K^+, CX_3, and Y^-. Because *three* particles could be formed in the reaction, the CM velocities are not necessarily opposed, and the velocity of the dissociating Y^- could be orientation dependent with respect to the incoming K^+. For heads orientation, where the K attacks the Y end, the Y^- could be ejected *toward* the incoming K^+ with an antiparallel velocity; for tails orientation the Y^- could be ejected *away* from the incoming K^+ with a parallel velocity. The escape of the ions from one another could thus be orientation dependent, being more facile in the heads orientation where the velocities are antiparallel. The preliminary data with oriented molecules were thus interpreted mainly as this exit-channel effect.

The present results are obtained with a greater signal-to-noise ratio which has allowed us to make more quantitative measurements at energies down to threshold. The present results agree with the earlier results and now show that the reactivity of the tails orientation completely disappears at low energies.[16] Heads and tails have different energetic thresholds. For CF_3Br the heads/tails thresholds are 3.4 and 4.0 eV, respectively, which, combined with the negative ion studies of Compton et al.,[17] can be interpreted as thresholds for formation of CF_3Br^- and $CF_3 + Br^-$, respectively. Above 4 eV, three products are formed, and the exit channel interaction can be orientation dependent as previously described. But, in the narrow energy range $3.4 \le E \le 4.0$ eV, only the parent ion, CF_3Br^-, is formed, so only two particles emerge from the collision. Strongly orientation-dependent exit channel interactions are thus expected to be absent, and the orientation dependence is interpreted as mainly an entrance channel interaction, which is expected to be the electron transfer. The orientation dependence is thus interpreted as a preference for the electron to be transferred to the Br end of CF_3Br. The electron transfer should also be characteristic of lower (thermal) energies where the ions cannot be separated, suggesting that the conclusions drawn about electron transfer in these hyperthermal energy experiments are extensible to thermal energies as well.

Threshold differences are also observed for CH_3Br and CF_3Cl, suggesting similar behavior, but the product ions have not yet been identified.

II. Experimental Section

The experimental apparatus has been described.[14,18] Unlike previous experiments,[14] the CX_3Y molecules are seeded in helium (CX_3Y:He ≈ 1:9) at ≈80 Torr to cool the beam, with low stagnation pressure being used to avoid formation of clusters in the beam. The CX_3Y beam is passed through an inhomogeneous electric hexapole field 140 cm long which passes molecules in states with $M \cdot K < 0$. These molecules then fly adiabatically into a region of uniform field ≈15 V/cm. Molecules in these selected states are oriented with respect to the direction of the weak field. The direction of the weak field can be reversed to present either the heads or tails end to the incoming beam of K atoms. Ionizing collisions between the fast K atoms and the oriented molecules produce K^+ ions which are detected by one of two channeltron particle multipliers located in the plane of the crossed beams. In these experiments better collimation of the K beam reduced the scattering of the primary beam from the channeltrons, thereby enormously reducing the background counts and making these refined measurements possible.

A. Molecular Orientation. The symmetric top molecules are described by the usual[19] quantum numbers, J, K, and M, representing the total angular momentum and its projections onto the molecular axis and space-fixed axis (the electric field). Both a vector model and first-order perturbation theory show that the rotationally averaged orientation is

$$\varrho \equiv \langle\cos\theta\rangle = M \cdot K/J(J+1) \tag{4}$$

where θ is the angle between the molecular dipole μ and the external field $\mathbf{E}$. But at any instant, the probability of finding a molecule (in state $|JKM\rangle$) with a specific orientation with respect to the electric field is[20]

$$P_{JKM}(\varrho)\, d\varrho = 4\pi^2 |\psi_{JKM}|^2\, d\varrho \tag{5}$$

where $\varrho \equiv \cos\theta$. The orientation distribution function P_{JKM} can be written as a short expansion of Legendre polynomials.[20]

In an electric field, the energy shift of the top, W, is given by $W = -\mu \cdot \mathbf{E} = -\mu_0 E\langle\cos\theta\rangle$. Inside the hexapole field each molecule moves to minimize its energy and molecules with $\langle\cos\theta\rangle < 0$ are focussed because $|E| = 0$ on the axis. The transmission probability, $F_{JKM}(V_0)$, depends on the molecule and geometrical parameters of the field such as length of the field and size of any collimating apertures. For the present studies, a large exit aperture was used to maximize beam intensity, resulting in a range of $|JKM\rangle$ states, although for each state selected $M \cdot K < 0$.

The final orientation distribution function, $P(\varrho,V_0)$, of the molecules in the transmitted beam is a superposition[21] of the various $|JKM\rangle$

(14) (a) Brooks, P. R.; Harland, P. W.; Phillips, L. F.; Carman, H. S., Jr. *J. Phys. Chem.* **1992**, *96*, 1557−1561. (b) Harland, P. W.; Carman, H. S., Jr.; Phillips, L. F.; Brooks, P. R. *J. Phys. Chem.* **1991**, *95*, 8137−8142. (c) Harland, P. W.; Carman, H. S., Jr.; Phillips, L. F.; Brooks, P. R. *J. Chem. Phys.* **1990**, *93*, 1089−1097. (d) Harland, P. W.; Carman, H. S., Jr.; Phillips, L. F.; Brooks, P. R. *J. Chem. Phys.* **1989**, *90*, 5201−5203.

(15) For reviews of collisional ionization, see: (a) Kleyn, A. W.; Los, J.; Gislason, E. A. *Phys. Rep.* **1982**, *90*, 1. (b) Lacmann, K. *Potential Energy Surfaces*; Lawley, K. P., Ed.; John Wiley: New York, 1980; p 513. (c) Baede, A. P. M. *Adv. Chem. Phys.* **1975**, *30*, 463. (d) Los, J.; Kleyn, A. W. *Alkali Halide Vapors*; Davidovits, P., McFadden, D. L., Eds.; Academic Press: New York, 1979; p 279.

(16) Xing, G.; Kasai, T.; Brooks, P. R. *J. Am. Chem. Soc.* **1994**, *116*, 7421−22.

(17) Compton, R. N.; Reinhardt, P. W.; Cooper, C. D. *J. Chem. Phys.* **1978**, *68*, 4360−4367.

(18) Xing, G. Ph.D. Thesis, Rice University, 1993.

(19) Townes, C. H.; Schawlow, A. L. *Microwave Spectroscopy*; Dover: New York, 1975.

(20) (a) Stolte, S. *Ber. Bunsenges. Phys. Chem.* **1982**, *86*, 413−421. (b) Choi, S. E.; Bernstein, R. B. *J. Chem. Phys.* **1986**, *85*, 150−161.

(21) Brooks, P. R. *J. Phys. Chem.* **1993**, *97*, 2153−2157.

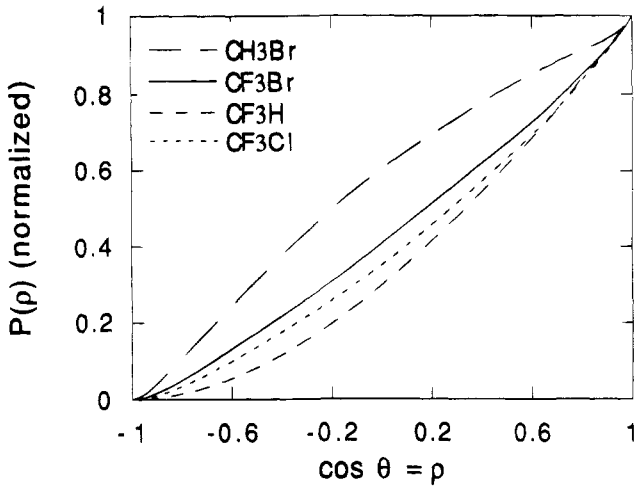

Figure 1. Distribution of the orientations of molecules state selected by the inhomogeneous hexapole electric field.

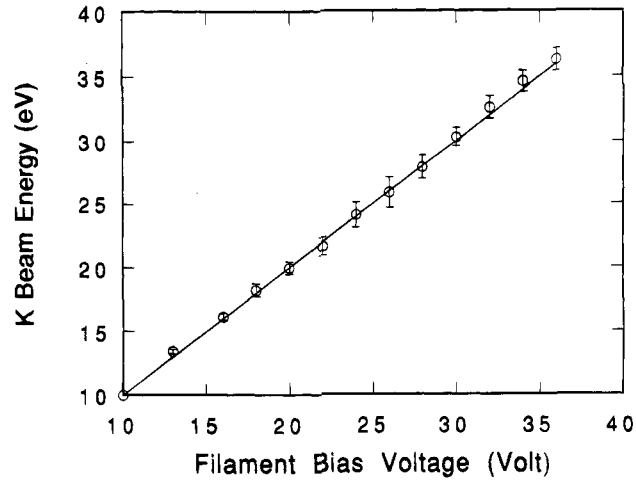

Figure 2. K beam energy vs bias voltage. Solid line: $E = V$.

probabilities weighted with the hexapole transmission function F and the Boltzmann probability, $f_{JK}(T)$, of populating state $|JKM\rangle$ at low rotational temperature T:

$$P(\varrho,V_0) = A \sum_{J} \sum_{K=1}^{J} \sum_{M=1}^{J} P_{JKM}(\varrho)\, f_{JK}(T)\, F_{JKM}(V_0) \quad (6)$$

$P(\varrho,V_0)$ is calculated and shown in Figure 1 for a focussing voltage of $V_0 = \pm 8$ kV, the conditions under which the data were taken. The probability distribution, $P(\varrho)$, is sensitive to the molecule because the Boltzmann state distribution differs from molecule to molecule, but $P(\varrho)$ is remarkably insensitive to the focussing voltage and the rotational temperature. This insensitivity to V_0 and T_{rot} and the monotonic dependence on ϱ is a consequence of the large exit aperture used. The calculated $P(\varrho)$ distribution becomes non-monotonic and sensitive to V_0 if the aperture is decreased (in the calculations) to make the diameter comparable to the deflection of the molecules in the hexapole field. Under these assumed circumstances the probability of transmission is highly dependent upon ϱ and molecules in single quantum states can be selected.[5c,d,7]

B. Fast K Atoms. The fast K atom beam is generated by resonant charge exchange inside the K oven.[22] The K reservoir is heated to ≈100 °C and K atoms are surface ionized on a hot W wire inside the oven biased at potential V. The K^+ ions are accelerated to a grid at ground potential ≈1 mm away from the filament. The energetic K^+ ions, with kinetic energy nominally equal to V electronvolts, drift through the K vapor in the oven and undergo resonant charge transfer with negligible momentum loss to form a neutral K atom beam, also with nominal energy V. Residual ions are deflected out of the beam by charged deflector plates outside of the oven. The resulting neutral beam crosses the beam of oriented molecules at right angles and consists of fast K atoms with a small fraction of thermal energy K atoms. The thermal atoms lack sufficient energy to cause ionization and make no contribution to the signal.

Because of contact potentials inside the oven, the actual K beam energy differs by a few electronvolts from the nominal filament−grid voltage difference, and space charge and the finite acceleration region broaden the energy distribution in the K beam. To determine the actual translational energy of the K atoms, the beam was chopped with a 400 Hz wheel to produce 10 μs beam pulses and the time-of-flight distribution of the atoms was measured over a flight path of ≈50 cm. The measured beam energy was determined to be identical to the filament bias voltage V to within 2% as shown in Figure 2. This fortuitous relationship is apparently the result of contact potentials cancelling the voltage drop to the center of the heated filament (≈3 V). The width of the energy distribution $\Delta E/E \approx 4\%$. (In view of the voltage drop along the filament, the relatively narrow energy distribution may result as a consequence of the restriction of the effective region of ionization by the small solid angle of extraction of the fast neutral beam and a preference for surface ionization of the atoms to occur in the center of the filament.) The calibration of the K beam energy was independently checked by determining the energy threshold for the unoriented reaction

$$K + SF_6 \rightarrow K^+ + SF_6^- \quad (7)$$

as described later. The energy in the center of mass system is given by

$$E_{cm} = \frac{M}{M + M_K}(E_K + E_0) \quad (8)$$

where M is the mass of the gas molecule, M_K that of potassium, E_K the lab energy of the fast potassium atoms, and E_0 a small correction for the speed of the gas molecule.[23]

The K beam intensity, I_K, was monitored by surface ionization on a cool filament ≈50 cm from the reaction center, but the detection efficiency was observed to be sensitive to the surface condition of the filament and to the beam energy. The intensity of fast neutral atoms is proportional to the intensity of ions inside the oven, which in the space charge limit is proportional to $E^{3/2}$. Thus the neutral intensity is expected to be proportional to $E^{3/2}$, as experimentally observed by Aten and Los,[24] and roughly confirmed here. The space charge limited relationship, $I_K \propto E^{3/2}$, is used here to normalize the ion signals at different K beam energies, but the (erroneous) measured intensity was used earlier[14].

C. Ion Detection. The local electric field determines the direction in which the CX_3Y molecules are oriented, but that field also deflects the ions produced in the collision. In order to be able to change the orientation (by changing the direction of the field) while still detecting positive ions, two channeltron particle multipliers were used, with one detecting positive ions in the heads electric field configuration and the other detecting positive ions in the tails configuration. See refs 14 and 18 for details concerning corrections for relative collection efficiency and signal analyses.

III. Results

A. Cross Sections. Collisional ionization was studied for reactions of K atoms with CF_3Br, CH_3Br, CF_3Cl, and CF_3H. (The signals decreased in that order and consequently the CF_3-

(22) Helbing, R. K. B.; Rothe, E. *Rev. Sci. Instrum.* **1968**, *39*, 1948–1950.

(23) For beams crossing at right angles, $E_{cm} = {}^1/_2\mu v_r^2 = {}^1/_2\mu(v_K^2 + v_G^2)$, where μ is the reduced mass $MM_K/(M + M_K)$, and v the velocities of K and gas. v_G is assumed to be the terminal speed of a 10% mixture of the gas in He for which the flow velocity is given by conservation of energy, ${}^1/_2mu^2 = \int C_P\, dT$, where m and C_P are the average mass and average heat capacity, respectively. From this calculation E_0 was determined to be 0.17, 0.22, 0.27, and 0.21 eV for CF_3Br, CF_3Cl, CF_3H, and CH_3Br, respectively. SF_6 was not accelerated and E_0 was neglected.

(24) Aten, J.; Los, J. *J. Phys. E* **1975**, *8*, 408.

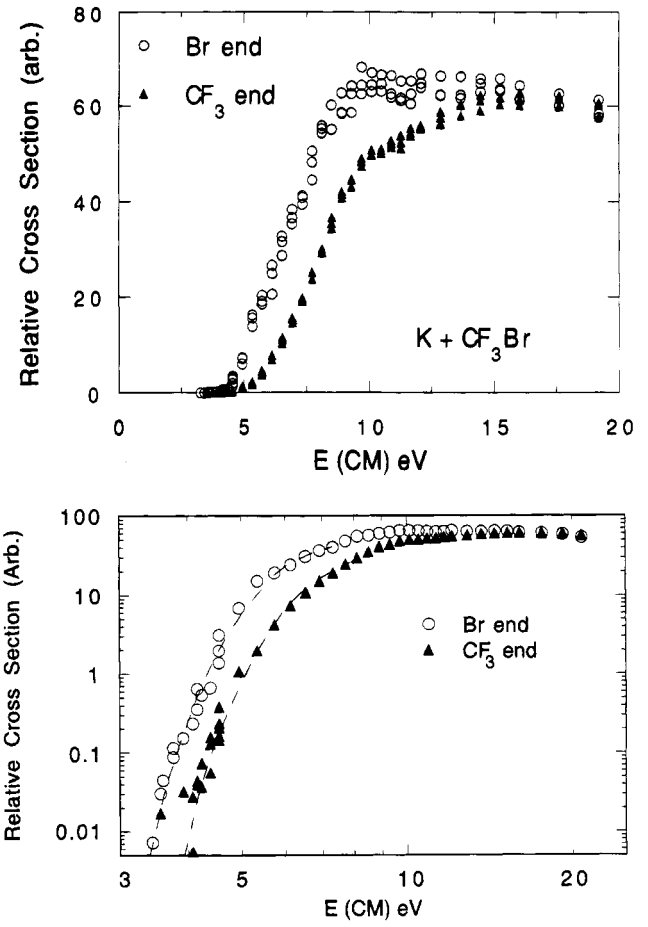

Figure 3. (a, top) Relative cross section (positive ion signal/K beam intensity) for oriented CF_3Br vs CM kinetic energy. Solid symbols represent attack at the negative end of the molecule. (b, bottom) log–log presentation of data in part a.

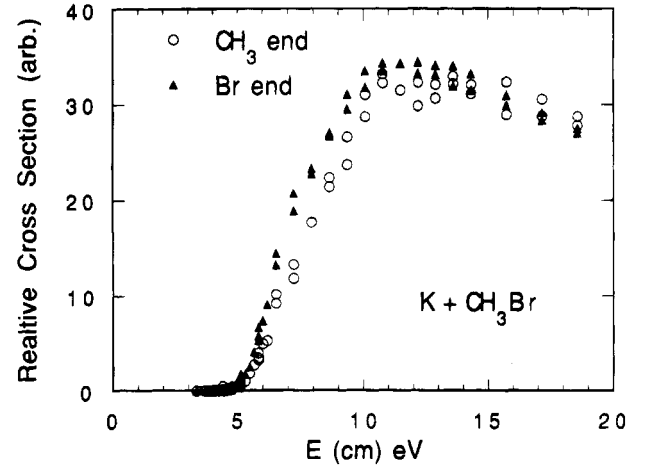

Figure 4. Relative cross section (positive ion signal/K beam intensity) for oriented CH_3Br vs CM kinetic energy. Solid symbols represent attack at the negative end of the molecule.

Br and CH_3Br systems were more thoroughly explored and are emphasized in this report.) The effect of orientation is readily apparent as can be seen in plots of the relative cross section vs CM energy, Figures 3–6. The relative cross section is the corrected K^+ ion signal S_{K^+} divided by K intensity, S_{K^+}/I_K, where $I_K \propto E^{3/2}$. The polarity of the end under attack is determined by the direction of the uniform electric field. (The state selected molecules are in states in which the energy increases with field: the positive end of the dipole points toward the positive field plate.) In Figures 3–6 the symbols denote the *polarity* of

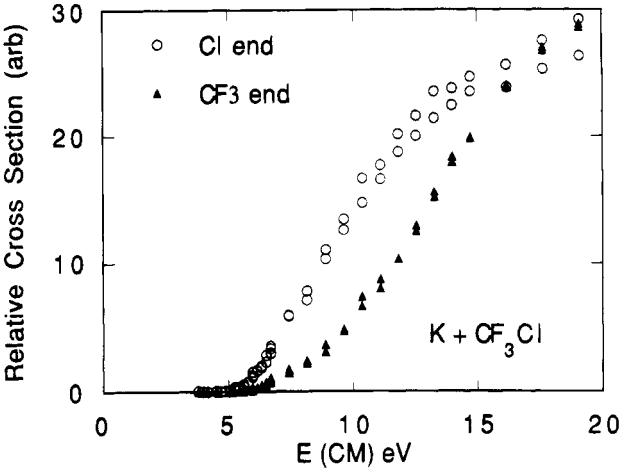

Figure 5. Relative cross sections for oriented CF_3Cl. Solid symbols denote attack at the negative end of the molecule.

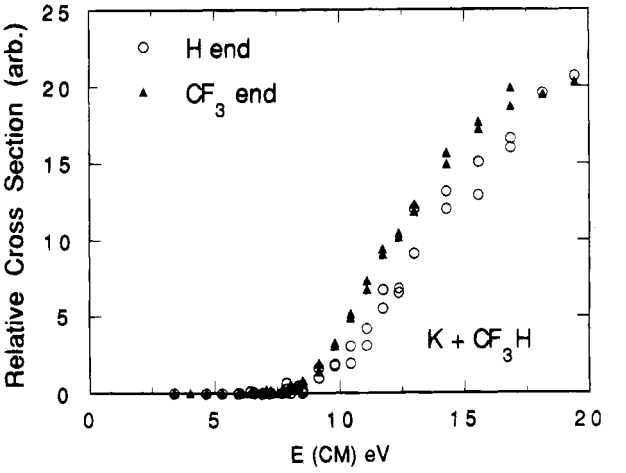

Figure 6. Relative cross sections for oriented CF_3H. Solid symbols denote attack at the negative end of the molecule.

the end under attack: open symbols denote positive end attack; closed symbols denote negative end attack. Although the direction of the molecular dipole must be known in order to determine which end is positive or negative, we surmise, on the basis of the high electronegativity of Br, that in CH_3Br the Br is negative. In CF_3Br, dipole moment trends, electronegativities, and reactivity strongly suggest that the Br end is positive, which is supported by similar data[5a] for CF_3I and a direct measurement on CF_3I.[25] We conclude that for both CF_3Br and CH_3Br the Br end is the more reactive end. Similar reasoning suggests that Cl is the reactive end of CF_3Cl. In all cases the experiments unambiguously establish the polarity of the more reactive end.

Regardless of the direction of the dipole moment, it is clear from Figures 3–6 that molecular orientation has a significant effect on the reactivity. The more reactive ends of CF_3Br and CH_3Br have different polarity, showing not only that this is a real molecular effect but also that the electron is not simply transferred to the positive end of the dipole. These conclusions are similar to those reached from our preliminary studies[14c] on CF_3I/CH_3I and are reinforced by the absence of any effect for SF_6 which is a spherical top and cannot display any asymmetry. (See Figure12, below.)

B. The Steric Effect. Because the relative cross section varies strongly with energy, it has been convenient to divide

(25) Gandhi, S. R.; Bernstein, R. B. *J. Chem. Phys.* **1988**, *88*, 1472–1473.

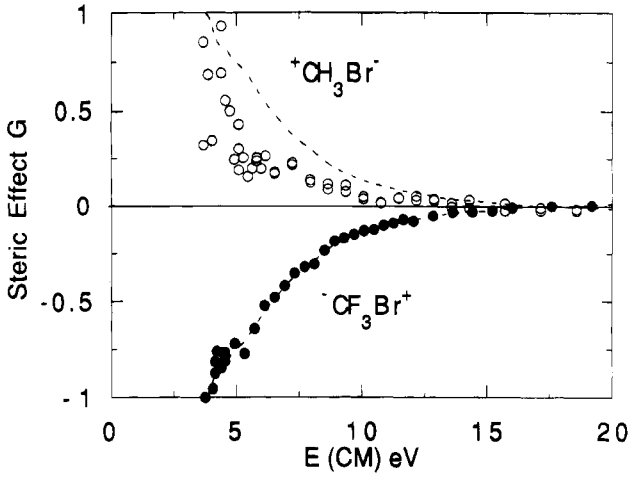

Figure 7. Experimental steric effect plotted vs E for K reacting with the various molecules shown. The dashed line is the negative of the smooth curve passing through the CF_3Br data.

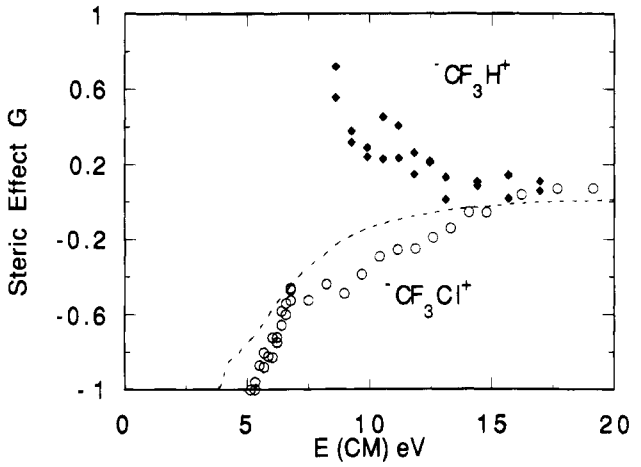

Figure 8. Experimental steric effect. The dashed line is the smooth curve which passes through the CF_3Br data in Figure 7.

out this variation by defining the steric effect G as

$$G = \frac{S_- - S_+}{S_- + S_+} \tag{9}$$

where S_-, S_+ are the signals for attack at the negative or positive end of the molecule.[26] If the reactivity is independent of orientation, $S_- = S_+$ and $G = 0$. On the other hand, if one end is completely unreactive, $G = \pm 1$, the sign depending on whether the negative or positive end is more reactive. This steric effect is shown in Figures 7 and 8. As suggested in our preliminary data $|G|$ approaches zero with increasing energy and the steric effect disappears at $E \approx 20$ eV. For CF_3Br, CF_3Cl, and CH_3Br the steric effect can clearly be extrapolated to ± 1, showing that at low energies only *one end* of each of these molecules is reactive. In each case it is the heads (Br or Cl) end that remains reactive.

C. Energy Thresholds. The steric effect, G, approaches ± 1 at low energies so the reactivity of one end of the molecule must disappear at low energies. The measurements of G thus demonstrate that different ends of these molecules have different thresholds, as was suggested in the rough preliminary experiments. The behavior at threshold was therefore studied in detail and these data are shown in Figures 9–11. Similar data are not shown for fluoroform, CF_3H, because the threshold was at

(26) This is the same quantity defined in preliminary work (ref 14) but with a slightly different nomenclature.

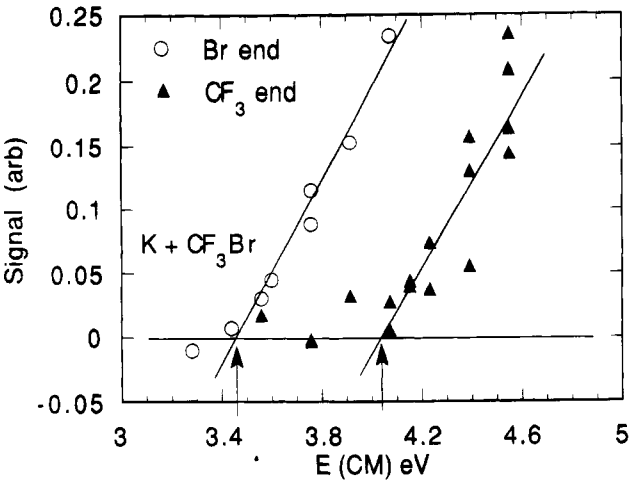

Figure 9. Signal vs energy near threshold for K + CF_3Br. Open symbols denote attack at the positive end of the molecule; closed symbols denote attack at the negative end. Arrows at 3.45 and 3.97 eV denote thresholds for formation of CF_3Br^- and Br^- + CF_3.

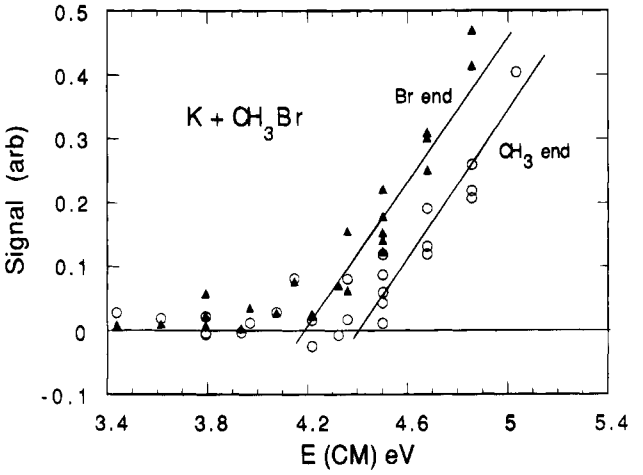

Figure 10. Threshold behavior of CH_3Br. The identity of the negative ions has not been reported.

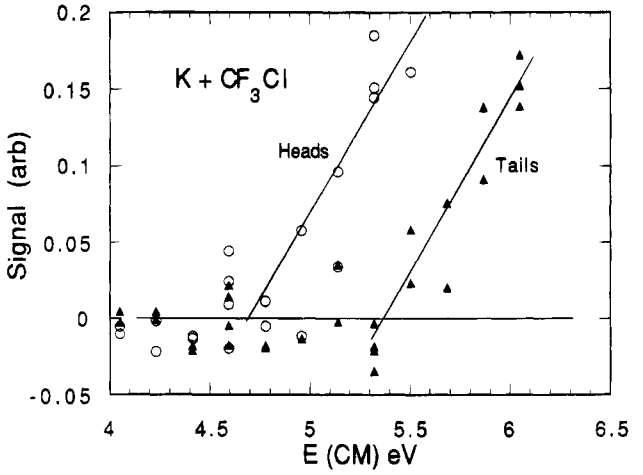

Figure 11. Threshold behavior of CF_3Cl. The identity of the negative ions has not been reported.

lab energies, ≈12 eV, where the background was high, yielding a lower signal/noise and scattered data points. The *apparent* thresholds are determined by linear extrapolation from these plots and are listed in Table 1. The absolute thresholds are not well-determined because the threshold law is not known and the energy spread is not extensively characterized. But since the cross sections are similar over a large range (Figure 3), the

Table 1. Experimental Energy Thresholds (CM) for Collisional Ionization of K Atoms with Oriented Molecules

	E_{th} (eV)[a]			
	CF_3Br	CH_3Br	CF_3Cl	CF_3H
heads	3.4	4.2	4.7	≤8.3
tails	4.0	4.4	5.4	≤7.9

[a] Uncertainties are ≈±0.2 eV, except for CF_3H where the uncertainty is ≈±0.4 eV.

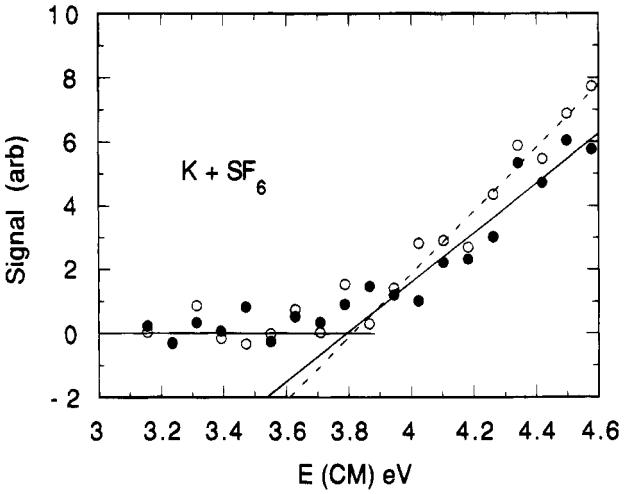

Figure 12. Threshold data for SF_6. Comparable literature values suggest the apparent threshold should be 3.8 ± 0.2 eV.

threshold laws for both orientations are expected to be similar. Thus the threshold difference is expected to be better determined.

As described previously,[14] weak beams of SF_6 are transmitted through the hexapole field at zero voltage. Because SF_6 is a spherical top with no orientational asymmetry, it has no permanent dipole moment, and it is unaffected by the high voltage. The experimental signals for SF_6 were thus used to account for differences in ion collection and detection efficiency. In order to check the energy calibration, the threshold for ionization was also measured and is shown in Figure 12. Least-square fits to the data above zero extrapolate to essentially the same threshold (3.75 eV) for the two electric field configurations, in good agreement with similar values from the literature,[27] 3.8 ± 0.2 eV. (Different slopes for the different "orientations" reflect different ion collection and detection efficiencies for the different channeltrons. The data for other molecules were corrected for the different efficiencies by using the SF_6 data.)

IV. Discussion

A. Thresholds. The observation of different thresholds for heads and tails orientations shows that at very low energies reaction is confined to *only one end* of the molecule. We directly observe that there is no reaction for attack in the unfavored orientation.

Different thresholds for attack at different "ends" of these molecules require the final state of the system, at the respective thresholds, to be somehow different for attack at the opposite ends of the molecule. For CF_3Br we believe that different *products* may be formed, depending on the end attacked, but the same species in different internal (say vibrational) states could also be a possibility.

In these experiments only the positive ion, assumed to be K^+, was detected and there are two likely low-energy reaction channels:

$$K + CX_3Y \rightarrow K^+ + Y^- + CX_3 \qquad (10a)$$

$$\rightarrow K^+ + CX_3Y^- \qquad (10b)$$

(KY salt molecules might be formed, but since only charged particles are detected, the neutrals would not be observed.) At energies a few volts above threshold, the fragmentation reaction 10a accounts for ≈95% of the products[17] and the early experiments were interpreted on the basis of reaction 10a. At sufficiently low energies, however, the parent ion may not have enough energy to fragment and reaction 10b can be dominant.

i. CF_3Br. The negative ions formed in collisions of Na atoms with unoriented CF_3Br have been studied, together with their thresholds, by Compton, Reinhardt, Cooper.[17] They observed the parent ion, CF_3Br^-, and determined the vertical electron affinity, EA_v, to be 0.91 ± 0.2 eV. From the threshold for appearance of the Br^- ion, the bond strength of the negative molecular ion, $D(CF_3-Br^-)$, was determined to be 0.54 eV. From these data and the ionization potential of K (4.34 eV) one can calculate a threshold: IP(K) − EA(CF_3Br) = 3.43 eV for electron transfer to CF_3Br to give the parent ion

$$K + CF_3Br \rightarrow K^+ + CF_3Br^- \qquad (10b')$$

At higher energies, the negative molecular ion can fragment,[17] giving

$$K + CF_3Br \rightarrow K^+ + Br^- + CF_3 \qquad (10a')$$

with threshold = IP(K) − EA(Br)[28] + $D(CF_3-Br)$[29] = 4.34 −3.36 + 2.99 = 3.97 eV.

These threshold energies for formation of the parent ion, CF_3Br^-, and for fragmentation into CF_3 and Br^- agree closely with the thresholds obtained for the oriented molecules listed in Table 1. (These energies are comparable because they are obtained from similar experiments.) We thus conclude that, at the lower (heads) threshold, parent CF_3Br^- is produced, and it is produced by attack at the Br end of the molecule. At the higher (tails) threshold, tail end attack results in fragmentation and produces Br^- fragments. Formation of the parent negative molecular ion by tails attack is apparently prevented by some barrier which can be overcome with ≈0.5 eV of translational energy. But the CF_3Br^- molecular ion is too weakly bound to accommodate this much energy, and the negative molecular ion breaks up according to reaction 10a'. (Above the tails threshold, heads attack probably also produces Br^- fragments because enough energy would likely be deposited in the parent ion to cause it to break apart. Above about 5 eV, Br^- is the dominant negative ion.)

These data thus suggest that different products are formed by attack at different ends of the molecule, which are manifested here by different energetic thresholds for the two orientations. In similar experiments, Aitken, Blunt, Harland[30] have recently discovered that electron bombardment of oriented CH_3Cl produces more parent CH_3Cl^+ for attack at the CH_3 end of the

(27) Leffert, C. B.; Tang, S. Y.; Rothe, E. W.; Cheny, T. C. *J. Chem. Phys.* **1974**, *61*, 4929. Hubers, M. M.; Los, J. *Chem. Phys.* **1975**, *10*, 235. Compton, R. N.; Reinhardt, P. W.; Cooper, C. D. *J. Chem. Phys.* **1978**, *68*, 2023−2036. The presently accepted value of EA(SF_6) is 1.05 eV (ref 29) which predicts a threshold of ≈3.3 eV. This suggests either that there is some sort of barrier to electron transfer or that the.linear extrapolation is inadequate for the collisional ionization experiments.

(28) EA(Br) = 3.364 eV: Hotop, H.; Lineberger, W. C. *J. Phys. Chem. Ref. Data Ser.* **1975**, *4*, 539.

(29) $D(CF_3-Br)$ = 3.06 eV: *Handbook of Chemistry & Physics*, 72nd ed.; Lide, D. R., Ed.; Chemical Rubber Co., Boca Raton, FL, 1991. $D(CF_3-Br)$ 2.99 eV from ref 17.

(30) Aitken, C. G.; Blunt, D. A.; Harland, P. W. *J. Chem Phys.* **1994**, *101*, 11074.

Table 2. Calculated and Experimental Thresholds (Random Orientations)

reaction	products			bond energy (eV)[a]	EA[b] (eV)	threshold (eV) calcd	threshold (eV) other exp[c]
$K + CF_3Br$	K^+		$[CF_3Br]^-$		0.91	3.43	3.43[f]
	K^+	CF_3	Br^-	3.06 (2.99[c])	3.36	4.04 (3.97)	3.97[f]
	K^+	Br	CF_3^-	3.06	1.85[d]	5.55	
	K^+	CF_2Br	F^-	(5.33)[e]	3.45	6.22	
$K + CF_3Cl$	K^+	CF_3	Cl^-	3.73	3.6	4.48	
	K^+	Cl	CF_3^-	3.73	1.85	6.23	
	K^+	CF_2Cl	F^-	5.33	3.45	6.22	
$K + CH_3Br$	K^+	CH_3	Br^-	3.07	3.36	4.05	4.03; 4.8[g]
	K^+	Br	CH_3^-	3.07	0.08	7.33	
	K^+	CH_2Br	H^-	4.42	0.75	8.01	
$K + CF_3H$	K^+	CF_3	H^-	4.63	0.75	8.21	
	K^+	H	CF_3^-	4.63	1.85	7.12	
	K^+	CF_2H	F^-	5.46	3.45	6.35	

[a] McMillen, D. F.; Golden, D. M. *Annu. Rev. Phys. Chem.* **1982**, *33*, 493–533. [b] Reference 29. [c] Reference 17. [d] Lide, D. R., Ed. *Handbook of Chemistry & Physics*, 65th ed.; Chemical Rubber Co.: Boca Raton, FL, 1984. [e] Estimate. [f] Calculated value is derived from this datum. [g] Moutihno, A. M. C.; Aten, J. A.; Los, J. *Chem. Phys.* **1974**, *5*, 85–94.

molecule but that the formation of CH_3^+ seems to be independent of orientation.

ii. Other Molecules. Unfortunately, for the other molecules studied, less is known about the negative ions formed and their thresholds. It is, of course, tempting to speculate that different products are being formed for different orientations in a manner analogous to that for CF_3Br and for the electron bombardment experiments.

1. CH_3Br. The parent ion has not been observed in previous studies.[17,31] Nevertheless, Figures 7 and 10 show that only one end of the molecule, the Br end, is reactive at energies near threshold. The difference in thresholds is ≈0.2 eV, and the tails threshold is in rough agreement with the calculated threshold to produce Br^- and with the observations of Compton et al. for formation of Br^-. If the analogy with CF_3Br is pursued, these data indicate that the parent ion is bound only by ≈0.2 eV (±≈0.2 eV), suggesting that the parent may be so fragile that it might not be observed.

2. CF_3Cl. The parent ion has been observed,[32] and Figure 11 shows a clear *difference* between heads and tails thresholds of ≈0.6 eV. Again, the Cl end is more reactive and at low energies only Cl-end attack produces ions. However, the absolute threshold is in poorer agreement with that calculated, possibly a result of our weaker signals because the reaction cross section is smaller than that for CF_3Br. Thresholds for other possible reaction products are shown in Table 2, and these thresholds are too high to account for the experimental results. Extrapolation of the higher energy data in Figure 8 to $G = -1$ suggests a tails threshold of ≈5.1 eV, still higher than the expected value of 4.5 eV. This nominally higher threshold might reflect the greater uncertainty in the signals as well as the possibility that there is a barrier to fragmentation and the ions are not formed with zero energy. We believe that the threshold *difference* is significant and note that it is about the same as that for CF_3Br; further interpretation must be held in abeyance pending more information.

3. CF_3H. The negative (CF_3) end of the molecule is more reactive, and the threshold lies at larger laboratory energies (≈12 eV) where the background is high and the signal-to-noise ratio is small. At these high energies it seems unlikely that the parent ion is formed, and the observed attack at the CF_3 end might lead to the breaking of the weakest bond (C–H) and to the formation of CF_3^-. For CF_3H, the H end is the more labile end of the molecule, and it thus seems that tails attack is more productive, in contrast to the other molecules studied. The formation of F^- is predicted to have a smaller threshold because of the high electron affinity of the F atom, but formation of this product is unlikely because the C–F bond is so strong. It will be interesting to determine which negative ion is formed.

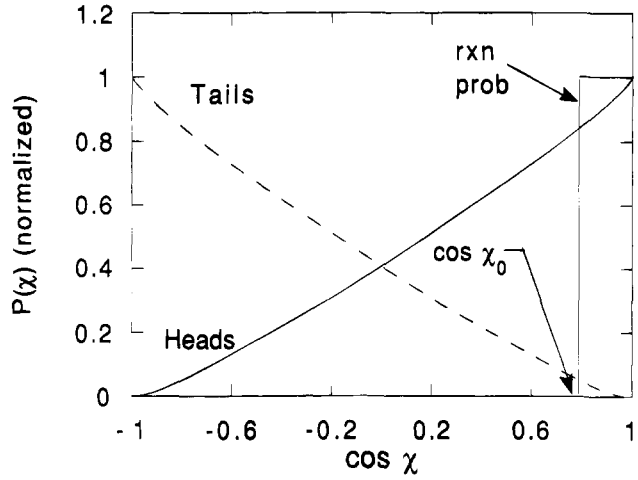

Figure 13. Probability distribution for CF_3Br in the heads and tails orientations. χ is the angle between the top axis and the initial velocity of the K atom. The step function on the right shows a reaction model with unit reaction probability within a cone of half angle χ_0 and its overlap with the heads and tails distributions (see also Figure 14).

B. The Steric Effect. The orientation of the molecules has a large effect on reactivity. This is especially remarkable considering that the molecules are not perfectly oriented, but instead they populate a number of rotational states which results in a distribution of orientations, as shown in Figure 1. The experimental comparison between heads and tails is effected by twisting the reference direction (the uniform electric field) by 180°. The distribution as seen by the incoming K atom is shown in Figure 13, where the CF_3Br probability distribution is plotted vs cos χ, where χ is the angle between the top axis and the initial asymptotic K velocity. Thus, if $\cos\chi = 1$ ($\chi = 0$), the K atom attacks the molecule at the Br end, and if $\cos\chi = -1$, the atom attacks the molecule at the CF_3 end. This distribution is so broad that in order to account for the large differences observed experimentally, the reactivity must be extremely sensitive to the angle of attack.

In order to see just how sensitive the reactivity is to orientation, we interpret the experimental steric factor G using

(31) McNamee, P. E.; Lacman, K.; Herschbach, D. R. *Faraday Discuss. Chem. Soc.* **1973**, *55*, 318–318.

(32) Hasegawa, A.; Williams, F. *Chem. Phys. Lett.* **1977**, *46*, 66–68.

(33) Other models are possible, but only one parameter can be extracted from the experimental data. This model is chosen for simplicity.

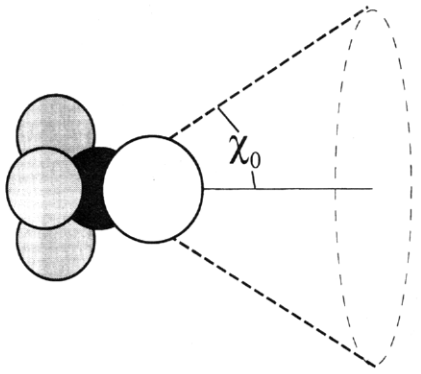

Figure 14. Schematic view of the reaction cone. The simple step-function model illustrated in Figure 13 suggests that atoms with initial velocities lying within the cone of half angle χ would react with unit probability, and velocities lying outside would not react.

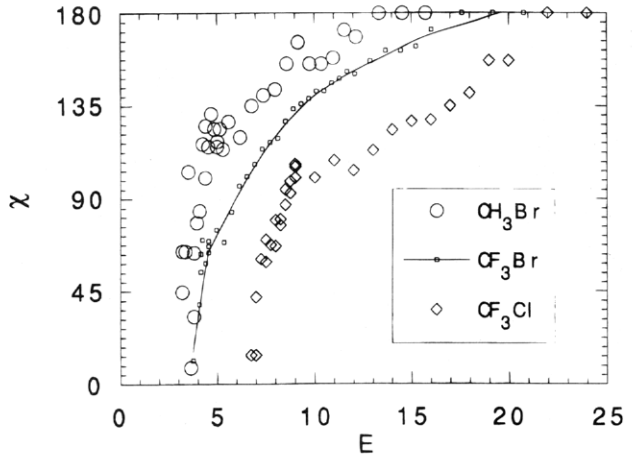

Figure 15. Half angle of reactive cone predicted by the step-function model of Figures 13 and 14, the calculated distributions of orientations of Figure 1, and the experimental values of G of Figures 7 and 8.

a simple step-function[33] model for reaction probability

$$P(\chi) = 1 \qquad \text{for } \chi \leq \chi_0 \tag{11a}$$

$$P(\chi) = 0 \qquad \text{for } \chi > \chi_0 \tag{11b}$$

where $P(\chi)$ is the probability of reaction for attack at angle χ and is sketched in Figure 13. In this model, an atom reacts if it approaches the molecule with initial velocity lying inside a cone of half-angle χ_0, as suggested[34] in Figure 14. The signal predicted by the model is proportional to the convolution of the step function with either the heads probability distribution or the tails probability distribution. A model value of G can then be calculated for various assumed values of χ_0 and an experimental estimate for χ_0 extracted by comparing the model and experimental values of G.

Values of χ_0 obtained from the experimental results using this model are shown in Figure 15. As anticipated, χ_0 is very small near threshold, suggesting that an almost collinear approach is required for reaction. As the reaction energy is increased, the cone of reaction becomes larger and larger until it envelops the entire molecule and the steric effect vanishes at energies ≈20 eV. Comparison between CF_3Br and CH_3Br, which have similar thresholds, shows a qualitative difference in the energy variation, with the methyl cone of reaction opening up very suddenly as the energy is increased. The CF_3Cl data are shifted to larger energy but with a shape similar to that of CF_3Br.

(34) The semantics are important here. We are only able to experimentally specify the direction of the quantization axis with respect to the velocity of the incoming atoms. An atom can follow a curved trajectory as it collides with the molecule, and χ_a, the angle between the *actual* velocity and the top axis, is unknown. Likewise, although we know which end of the molecule is under attack, we do not know the site of impact on the molecule.

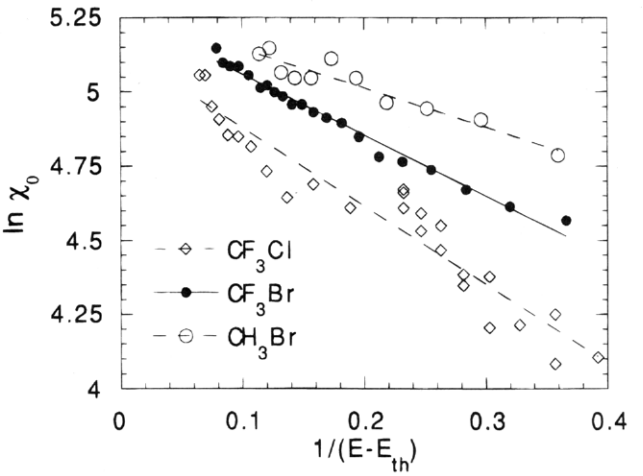

Figure 16. $\log_e \chi_0$ plotted vs $1/(E - E_{th})$ where $E_{th} = 3.4$, 4.2, and 4.7 eV for CF_3Br, CH_3Br, and CF_3Cl. Lines are least-square fits to the data. Data points at lower energies deviate from these fits.

The main conclusions here, that χ_0 is very small near threshold and then becomes larger and larger as the energy is increased, are essentially restatements of the experimental data and should not be dependent upon the reaction model. The variation of χ_0 with energy obviously shows that the steric effect varies with energy. Thus the amount of "steric hindrance" in a reaction (as well as the "steric factor") will also depend on energy, and should not be considered as a constant.

The energy dependence of the cutoff angle is roughly given by an Arrhenius-type of dependence,

$$\chi_0 \propto \exp\left(\frac{-B}{E - E_{th}}\right) \tag{12}$$

where E_{th} is the threshold energy and B is a parameter characterizing the decay, which is normally interpreted as the height of some potential barrier. Figure 16 shows a plot of ln χ_0 vs $1/(E - E_{th})$ for CF_3Br, CF_3Cl, and CH_3Br, together with least-square fits to the points. Values of B derived from these fits are respectively 2.05, 2.64, and 1.31 eV. Points near threshold were excluded from these determinations because they are less reliable and also more likely to include contributions from very low energy channels such as those forming the parent ion. These barrier values suggest that the hindering effect of the radical is the greatest for CF_3Cl, and the least for CH_3Br, and probably indicate the hindering effect of the R (CF_3 or CH_3) group on reaction to form Br^- or Cl^-. Identifying and measuring the orientation dependence of single product channels will help to clarify this point.

Earlier ESR studies suggest that the unpaired electron in CF_3X^- or CH_3X^- (X = Cl, Br, I) resides in an pσ^* antibonding orbital composed largely of the p orbitals of carbon and X, the unique halogen.[32] Our results suggest that the X end of the molecule is more accessible for the electron transfer, and transfer through the CF_3 or CH_3 end is apparently impeded by a potential barrier. Using CF_3Br as an example, this barrier is ≈0.6 eV and can be overcome by increasing the collision energy which then results in the fragmentation of the energized CF_3Br^- molecular ion.

V. Summary

Reactions involving an electron transfer from fast K atoms to oriented CF_3Br, CF_3Cl, and CH_3Br molecules have been

studied in crossed beams. More K^+ ions are produced when the K atom approaches the "heads" or more labile end of each molecule. The steric effect, $G = (S_- - S_+)/(S_- + S_+)$, where $S_\pm$ is the signal for attack at the positive or negative end of the dipole, approaches ± 1 at low energies, showing that reaction occurs only for attack at the Cl or Br end of the molecule. This is confirmed by threshold measurements: for CF_3X the energy threshold is $\approx$0.5 eV lower for heads attack than for tails attack. (For CH_3Br the difference is only $\approx$0.2 eV.) These data show that, near the lower threshold, reaction (to form K^+) occurs *only* for heads attack.

These data are interpreted in terms of a reaction model which assumes that reaction occurs only if the K atom is initially directed within a cone of half angle χ_0 on the heads end of the molecule. Values of χ_0 are extracted from the steric effect; at threshold, reactivity is confined to almost collinear configurations, and as the energy is increased the reaction cone opens up to include larger angles of attack. Steric requirements for these three reactions thus depend on the energy.

Our threshold for the heads orientation of CF_3Br agrees with the threshold[17] for the formation of the parent ion, CF_3Br^-, from randomly oriented CF_3Br. Likewise, our threshold for the tails orientation agrees with their threshold for formation of the fragment Br^-. We thus conclude that, near threshold, attack at the heads (Br) end forms CF_3Br^-. Formation of CF_3Br^- by tails attack is inhibited by a barrier of $\approx$0.5 eV, which can be overcome by increasing the collision energy, although when the barrier is surpassed, enough energy is deposited in the incipient CF_3Br^- to cause it to break up into CF_3 and Br^-.

Acknowledgment. Grateful acknowledgment is made to the Robert A. Welch Foundation and to the donors of the Petroleum Research Fund, administered by the American Chemical Society, for the support of this research. We thank the referees for constructive comments.

JA9432170